Space Launch System Ascent Static Aerodynamic Database Development

Jeremy T. Pinier[1]*, David W. Bennett[1]*, John A. Blevins[2]†
Gary E. Erickson[1]‡, Noah M. Favaregh[3]§, Heather P. Houlden[4]¶, and William G. Tomek[1]‡
[1]*NASA Langley Research Center, Hampton, VA, 23681*
[2]*NASA Marshall Space Flight Center, Huntsville, AL, 35811*
[3]*Analytical Mechanics Associates Inc., Hampton, VA, 23666*
[4]*ViGYAN Inc., Hampton, VA, 23666*

Notice to the Reader

The Space Launch System, including its predicted performance and certain other features and characteristics, have been defined by the U.S. Government to be Sensitive But Unclassified (SBU). Information deemed to be SBU requires special protection and may not be disclosed to an international audience, such as the audience that might be present at the 2014 AIAA SciTech Conference. To comply with SBU restrictions, details such as absolute values have been removed from some plots and figures in this paper. It is the opinion of the authors that despite these alterations, there is no loss of meaningful technical content. Analytical methodologies and capabilities are discussed; significant and interesting technical results are still present; and meaningful conclusions also presented.

This paper describes the wind tunnel testing work and data analysis required to characterize the static aerodynamic environment of NASA's Space Launch System (SLS) ascent portion of flight (Mach=0.3 to Mach=5). Scaled models of the SLS have been tested in transonic and supersonic wind tunnels to gather the high fidelity data that is used to build aerodynamic databases. A detailed description of the wind tunnel test that was conducted to produce the latest version of the database is presented, and a representative set of aerodynamic data is shown. The wind tunnel data quality remains very high, however some concerns with wall interference effects through transonic Mach numbers are also discussed. Post-processing and analysis of the wind tunnel dataset are crucial for the development of a formal ascent aerodynamics database.

*Research Aerospace Engineer, Configuration Aerodynamics Branch, MS 499, Senior Member AIAA.
†Aerospace Engineer, EV-33, Senior Member AIAA.
‡Research Aerospace Engineer, Configuration Aerodynamics Branch, MS 499.
§Research Engineer, 21 Enterprise Parkway Suite 300.
¶Research Engineer, 30 Research Drive.

Nomenclature

Symbols

A_{BL}	=	left booster base area
A_{BR}	=	right booster base area
A_C	=	core stage base area
AF	=	axial force
AFF	=	forebody axial force
$ALPHA$	=	body axis system angle of attack
$ALPHAV$	=	total angle of attack
$BETA$	=	body axis system sideslip angle
CAF	=	axial force coefficient, forebody
$CLLF$	=	rolling moment coefficient, forebody
$CLMF$	=	pitching moment coefficient, forebody
$CLNF$	=	yawing moment coefficient, forebody
CNF	=	normal force coefficient, forebody
CYF	=	side force coefficient, forebody
YM	=	yawing moment
YMF	=	forebody yawing moment
P_{BL}	=	left booster absolute base pressure
P_{BR}	=	right booster absolute base pressure
P_C	=	core stage absolute base pressure
P_{inf}	=	freestream static pressure
$PHIV$	=	roll angle
M	=	Mach number
Y_{BL}	=	distance from core stage centerline to left booster centerline
Y_{BR}	=	distance from core stage centerline to right booster centerline

Dedication

The authors would like to dedicate this present work to our late friend, colleague, and co-author Noah Favaregh, who recently passed away, much too early. Noah was not only an integral part of our aerodynamics team for the past 6 years at NASA Langley, but was also one of the most passionate and genuinely caring people. His constant striving for technical excellence made all of us around him better engineers. On top of being a great engineer with a bright future, Noah was a larger-than-life human being, husband, and father, who excelled at everything that he decided to put his energy in. We miss his presence every day, and will honor him by carrying his spirit with us in everything that we do.

Introduction

The Space Launch System (SLS) is NASA's future cargo and crew launch vehicle that is being designed for beyond low-Earth orbit missions. Its core stage is a modified Space Shuttle external tank fitted with 4 RS-25 liquid rocket engines as the main propulsion system. Two five-segment solid rocket boosters (SRB) provide additional thrust for the first two minutes of flight. There are various configurations of the SLS to accommodate for crew and cargo of various sizes, ranging from a 70 metric ton payload for the Block 1 version named SLS-10003, to the 130 metric ton payload to low-Earth orbit (LEO) for the Block 2 cargo-only version, named SLS-21003. The current paper describes the development of the ascent aerodynamic database for the SLS-10003 configuration only, even though many of the wind tunnel tests included testing of all SLS configurations, in the interest of efficiency. The primary source of data for developing the static aerodynamic databases for SLS is from wind tunnel testing of scaled launch vehicle models. To characterize

the aerodynamics of the vehicle over the entire ascent trajectory, test data needs to be obtained at Mach numbers ranging from low subsonic (≈0.3) to high supersonic (≈5). A description of the wind tunnel test that was conducted at the Boeing Polysonic Wind Tunnel (PSWT) to develop the current version of the ascent aerodynamic database will be presented in the first part. The second part of the paper will describe in detail the post-processing analysis that is performed with the wind tunnel data to result in a formal database that is used by the a number of disciplines: trajectory, guidance, navigation and controls, and loads analysis, primarily. The current version of the ascent aerodynamic database discussed in this paper is named SLS-10-D-AFA-003-rev1.

I. Wind Tunnel Testing

A. Boeing Polysonic Wind Tunnel Facility Description

Figure 1. SLS-10003 in the supersonic test section

The Boeing Polysonic Wind Tunnel (PSWT) in St Louis, Missouri, is an in-line, blow-down tunnel with a square 4×4 foot test section that uses a removable transonic test section cart to operate from $M = 0.45$ to 1.6. The cart is removed for testing in the higher supersonic range from $M = 1.6$ to 5.5. Figure 1 shows a picture of the SLS-10003 configuration in the supersonic test section. The facility operates mainly on a large gas turbine compressor that pumps air at a rate of 30 lb/s and a second back-up electric compressor can be brought online to provide an additional 15 lb/s, which proves useful to increase productivity. During subsonic and transonic operations ($0.5 \leq M \leq 1.6$) the removable transonic test section with perforated side walls is used to provide boundary layer suction, minimize shock and expansion wave reflections as well as wall interferences and provide a co-flow for easier start-up of the tunnel. Additionally, downstream ejectors provide the low pressure needed to start the tunnel without overloading the test article in the test section. Automatic control of plenum pressure as well as throttled flaps located in the diffuser allow for active control of Mach number. During supersonic operations ($1.5 \leq M \leq 4.5$), the transonic test section is removed to provide a solid wall test section, and a flexible plate nozzle allows adjustment of the throat area to control Mach number. In this mode, the start and un-start loads on the test articles are much higher. For this reason, force and moment balances with relatively large axial load limits (250 lbs) needed to be utilized. Since this wind tunnel is a blow-down open circuit tunnel, between 20 and 50 seconds of data can be acquired in one blow-down cycle, depending on the Mach number conditions. Data acquisition during pitch and roll polars is therefore performed continuously for efficiency (as opposed to pausing the model at each attitude where data is required) and digital low-pass filtering with a cut-off frequency on the order of 1 Hz is applied to the data to eliminate the fluctuations due to high frequency small oscillations of the model in the flow. The continuous pitch/roll sweep technique can present challenges when running at low static pressures (high

Mach numbers), in which case, pressure lags can occur in long lengths of tubing and therefore measurements can be corrupted. Special care was taken when designing the base pressure instrumentation for running continuous pitch sweeps to ensure that there was no significant lag in the measurements. One additional feature pertaining to the PSWT facility is its ability to perform Mach sweeps in the subsonic/transonic mode by actively controlling the main valve opening during the blow-down cycle. It was thus possible to acquire data during Mach sweeps from around $M = 0.4$ to 1.15 to study the transonic effects in detail. Mach polars are beneficial in identifying the potential effects of shock reflections occurring above Mach 1. PSWT Test number 904 was conducted in October of 2012 in this wind tunnel. Five different configurations of the SLS vehicle were tested since the front end of the model was designed to be modular. However, only the SLS-10003 configuration data is discussed and shown in the present paper. This wind tunnel dataset was the basis for the development of ascent aerodynamic database SLS-10-D-AFA-003-rev1 that is currently being used for flight simulations, guidance and navigation, controller development, and loads analysis.

B. Model Description

Tests at the outset of the SLS program were conducted at the NASA Marshall Space Flight Center's 14" Trisonic Wind Tunnel (TWT) on a 0.4%-scale model. This wind tunnel allows the aerodynamics team to acquire enough data in a short time to develop an initial aerodynamic database at a very low cost, that are used by the guidance, navigation and control (GNC) teams to design early trajectories and vehicle controls. The TWT also has a capability that allows the team to cover the entire Mach range, from low subsonic to high supersonic. The reader is referred to internal NASA reports by Mayle *et al.*,[1] and Crosby *et al.*[2] for details on these wind tunnel tests. To improve the fidelity of the outer mold line geometry, and consequently of the aerodynamic database model, larger scale testing was required. The scale of the model that was tested at the PSWT was 0.8%, resulting in an approximately 32"-long model. This scale is large enough to be able to manufacture the small protuberances on the outside of the model with appropriate fidelity, while small enough to collect quality data in a 4×4 foot test section wind tunnel, while minimizing the Mach range where shock reflection on the model can be a concern.

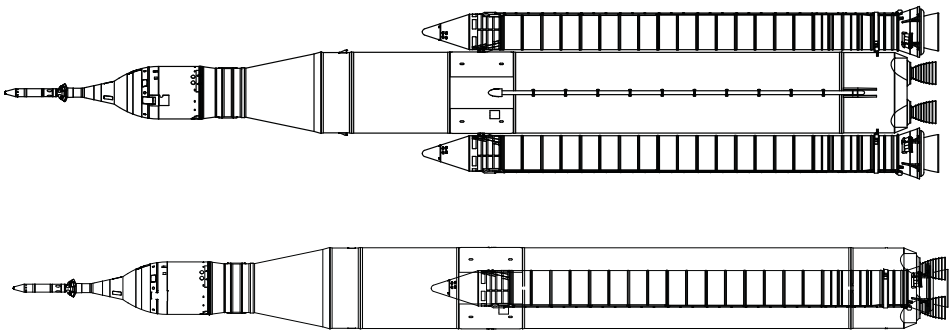

Figure 2. Top and Side views of the SLS-10003 configuration

Figure 2 shows a schematic of the SLS-10003 configuration as was tested during PSWT test 904. The model pictured in Fig. 1 was primarily built from aluminum to lower the weight and therefore minimize the oscillations and vibrations when subjected to unsteady flow, and tunnel start or un-start loads. Stainless steel was used for the high-precision parts including the balance adapter, by which the model is fastened to the balance.

Due to the presence of various protuberances (fuel feed lines, system tunnels, auxiliary booster motors, camera fairings, umbilicals, hold-down posts, etc), the outer mold line of the vehicle does not present any axes or planes of symmetry. Aerodynamic forces and moments should therefore not be expected to be symmetric, and no forcing of symmetry was applied to the data in the post-test analysis. It will be shown however that, due to the dominating presence of the solid rocket boosters (SRB), the forces and moments do present features of symmetry.

The wind tunnel Reynolds number based on the core stage diameter on this 0.8%-scale SLS model is around 2×10^6/ft, or two orders of magnitude below flight Reynolds number during most phases of ascent. The boundary layer therefore needed to be tripped to ensure transition to turbulence and a closer

Figure 3. View of the forward portion of the 0.8%-scale SLS-10003 wind tunnel model in the open Boeing PSWT test section. Boundary layer tripping strips are visible.

representation of the flight Reynolds number flow. However, slender bodies of revolution that are rolled during testing present a real challenge with respect to the placement of the transition grit or trip dots. After an investigation into that matter[3] using various transition grit patterns and qualitative diagnostic techniques such as sublimation, it was concluded that several circumferential trip dot strips with heights tailored to the Mach number range and applied to the model near the launch abort system tower would be sufficient to force transition to turbulence on the surface of the vehicle. This investigation, even though not fully conclusive as to the extent of the boundary layer transition effect, resulted in best practices that were developed during the Ares I Project, part of NASA's now-cancelled Constellation program. These best practices have been followed during SLS testing. More details about Ares I testing in the Boeing PSWT can be found in Pinier *et al.*[4] Figure 3 shows the location of the trip dot strips at two axial locations on the forward portion of the wind tunnel model and at one axial location on the conical nose of the solid rocket boosters.

C. Instrumentation

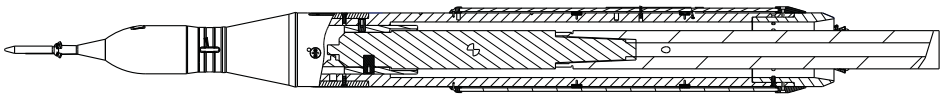

Figure 4. Cut-out view of the 0.8%-scale SLS-10003 wind tunnel model showing the sting and balance location within the model.

The model was mounted on a 6-component internal strain-gage balance (LaRC Balance 843B), with the balance moment center (BMC) placed near the estimated center of pressure location. The balance itself was mounted on a stainless steel (Vascomax) sting. Figure 4 shows the LaRC 843B balance mounted inside the SLS-10003 model and mounted into the front of the sting. Balance 843B is a recently-calibrated direct-read Langley balance and was chosen to match the expected loads during testing. Best practices related to the calibration and use of internal strain-gage balances as described by the AIAA Recommended Practices[5] were followed during SLS testing.

A total of eight static pressure tubes were run along the sting to measure the base pressure and the cavity pressure just inside the back end of the model. The core base pressure was measured using four averaged static pressure tubes installed diametrically opposed on the sting every 90^o. The SRB base pressure was measured using two pressure tubes per booster. The picture in Fig. 5 shows two of the four base pressure tubes on the top of the sting, and the booster base pressure tubes mounted on brackets to solidly keep them

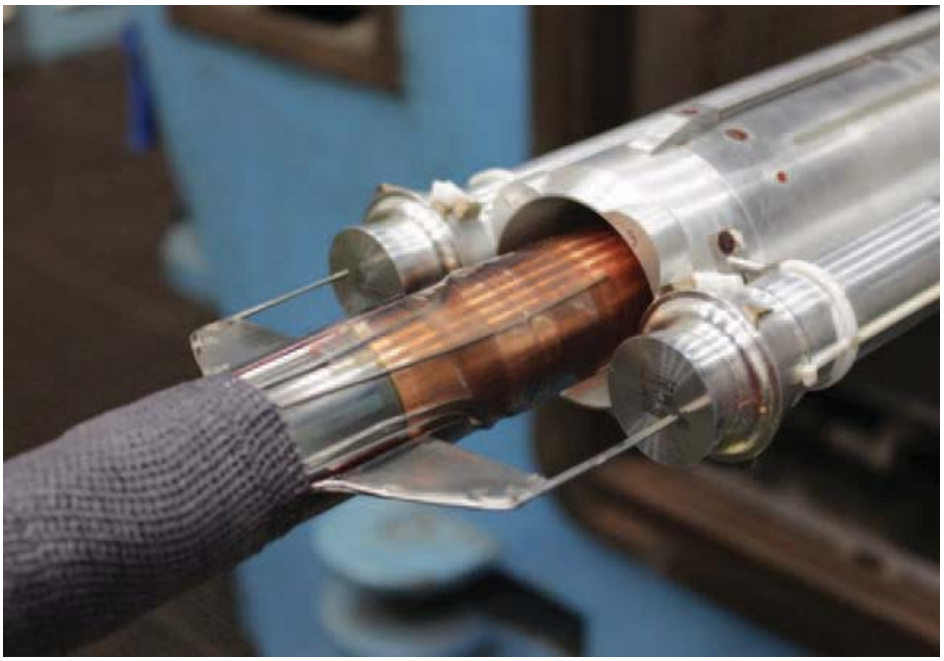

Figure 5. View of the base pressure measurements

in place. The booster pressure tubes do not touch the model. Electronically scanned pressure (ESP) modules were used as well as Kulite sensors to perform these measurements. Both were found to be comparatively reliable over the course of the test. The purpose of the base pressure measurements is to compute a base force on the core stage and both boosters that is used to correct the axial force and yawing moment as measured by the balance. This results in forebody forces and moments computed following these equations:

$$AFF = AF + (P_C - P_{inf}) * A_C + (P_{BL} - P_{inf}) * A_{BL} + (P_{BR} - P_{inf}) * A_{BR} \quad (1)$$

$$YMF = YM - (P_{BL} - P_{inf}) * A_{BL} * Y_{BL} + (P_{BR} - P_{inf}) * A_{BR} * Y_{BR} \quad (2)$$

A separate base force aerodynamic database is developed to account for the effects of the propulsion system, which are not modeled in the present wind tunnel test.

In rare cases of very high loads, the aft-end of the model could make contact, or foul, with the sting and corrupt the aerodynamic loads measured by the balance. Therefore, a fouling strip was installed to trigger a binary output and indicate compromised data. Overall, only very limited fouling was observed in the supersonic test section at relatively high angles-of-attack ($\alpha = 10 - 12$ degrees), where significant lateral as well as longitudinal dynamics were observed. In any instance where fouling was observed, the data was discarded at and around these data points.

The model/balance/sting assembly was mounted to the tunnel's support system which consisted of a 360-degree roll-coupler and an arc-sector in the pitch plane, with a center of rotation on the tunnel centerline close to the base of the model. This center of rotation enabled pitching the model over the required -12 to +12 degrees angle of attack while keeping the model near the center of the test section for optimal flow quality.

Schlieren flow visualization was utilized during the supersonic portion of testing where optical access is available. High-resolution images provide insight into the shock interactions, shock angles and, particularly, with regard to potential shock reflections back onto the model in the low-supersonic portion of testing. Figure 6 shows a schlieren flow visualization snapshot of the SLS-10003 configuration at a Mach number of 1.5, which is the low-end of the speed regime in the supersonic test section. It is observed that the model is free of reflected shocks at this Mach number and attitude. All configurations tested were inspected using the schlieren system to ensure that the data was not corrupted by shock reflection above M=1.5. In the transonic test section (below M=1.5) however, the schlieren system is not available due to the presence of perforated side walls that prevent optical access. The nature of the reflected shock and possible corruption of the data therefore has to be inferred from the aerodynamic measurements themselves.

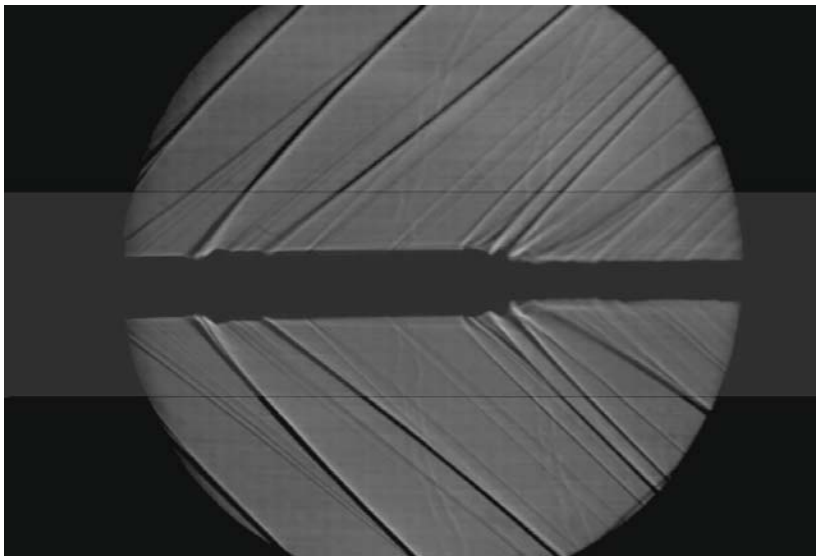

Figure 6. Schlieren flow visualization at Mach=1.5, $\alpha = 0$

D. Aerodynamic Data

The standard coordinate system used to post-process wind tunnel data and create databases is the body axis system, in which all forces and moments are tied to the wind tunnel model in all degrees of freedom. The aerodynamic data is however acquired in pitch and roll sweeps, as described in Section I.A. The data is therefore acquired in the missile axis system but then transferred to the body axis system. Figure 7 describes both axis systems. A significant amount of data was collected during this test to cover the required Mach number, angle of attack, and sideslip angle variable space. The following table summarizes the data runs that were acquired:

Test Parameter	Wind Tunnel Dataset
Mach number, M	0.50, 0.80, 0.90, 0.95, 1.05, 1.10, 1.20, 1.30, 1.50, 1.60, 2.00, 3.00, 4.00, 5.00
Pitch sweeps, ALPHAV	-12^o to +12^o continuous sweeps, at PHIV=0^o to 180^o every 45^o
Roll sweeps, PHIV	0^o to 360^o continuous sweeps, at ALPHAV=0^o, 2^o, 4^o, 8^o

Due to the large amount of data collected, only a small representative number of these data can be shown in this paper. All of the following plots show 6 degree-of-freedom (6-DOF) forebody forces and moments in the body axis system, as a function of ALPHAV, and PHIV.

1. Repeatability

With the goal of ensuring data quality throughout the test, repeatability assessments were performed at regular intervals during the test and were of two different types:

1. A reference set of runs was acquired initially and then at regular intervals during the test to ensure data consistency throughout the entire length of testing. Any long-term unexpected change in flow quality or any balance issue would be uncovered and investigated before any additional production runs were performed.

2. Uncertainty assessment repeat runs were also performed throughout the test to capture the dependency of data repeatability with all the variables. During post-processing, statistical methods are used to quantify repeatability, as used by Hemsch *et al.*[6] and Houlden *et al.*,[7] and following processes describes by Montgomery.[8] It is therefore important to gather repeatability data at various attitudes and flow conditions to detect any correlation in the residuals, in which case an uncertainty model can be built using this information.

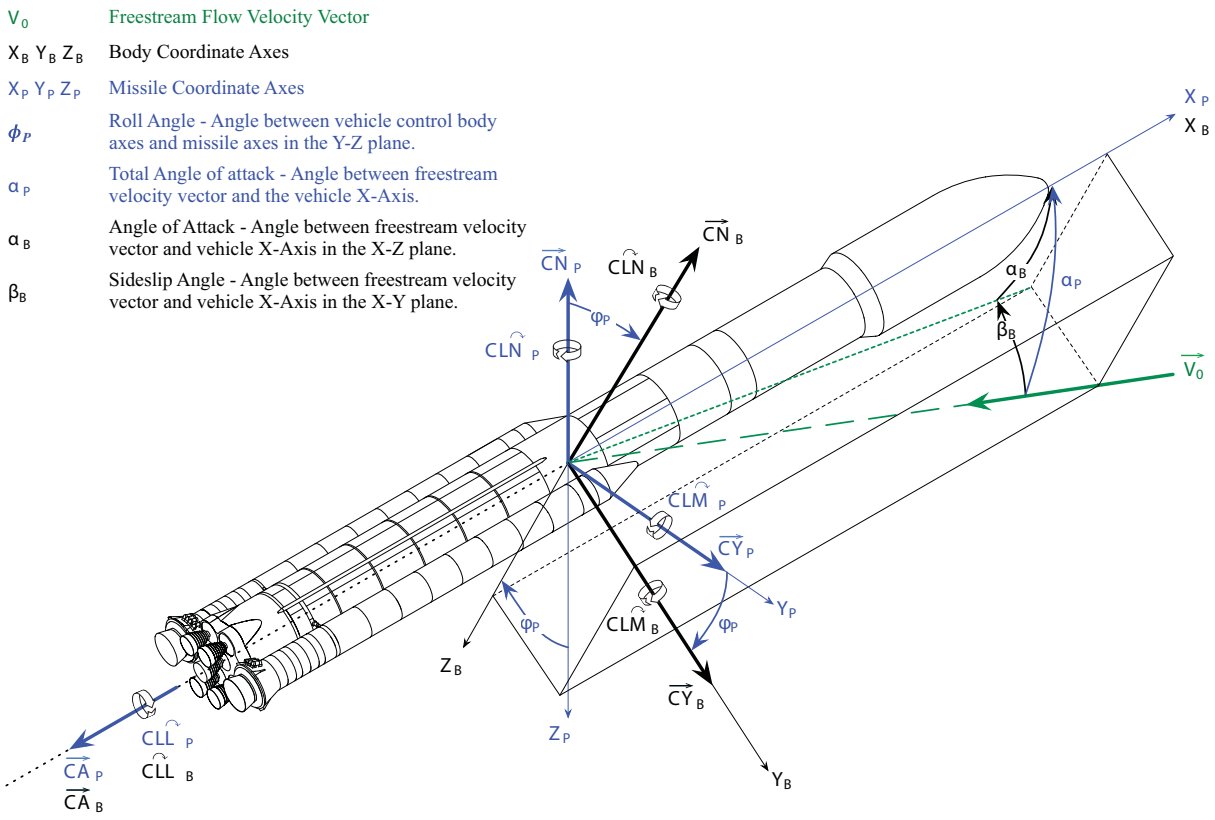

Figure 7. Definition of SLS coordinate systems

Balance calibration uncertainty is a result of the statistical curve fit error produced during balance calibration in the laboratory. It is therefore known before starting a test. For both types of repeats cited above, balance calibration uncertainty is used in real time as a measure of minimum uncertainty. Therefore, two repeat runs that do not fall within the balance calibration uncertainty bounds are not necessarily bad repeats, however, best practices and experience with these 6-component balances has shown that discrepancies between repeats should be expected to be either within the balance calibration uncertainty or on the same order of magnitude.

Figure 8 shows trends of the force and moment variations during three repeat pitch sweep runs at M= 0.5 and PHIV= 45^o. Figure 9 shows trends of the force and moment variations during two repeat roll sweep runs at M= 0.5 and ALPHAV= 8^o. Similarly, Figs. 10 and 11 show repeat pitch sweeps and roll sweeps (respectively) at M= 1.3. Since absolute magnitudes are not provided, the reader should focus on the magnitude of the discrepancies between repeat measurements relative to the total variation over a run, and the magnitude of the balance calibration uncertainty represented by the error bars. In all cases presented, repeat runs fell within the balance calibration uncertainty, indicating exceptionally good repeatability, considering that these runs are always performed in separate wind tunnel blows, and in some cases separated by multiple days.

All of the trends observed during testing, and shown in these plots are consistent with what would be expected on a launch vehicle of this type. In roll sweeps, the SRBs on each side of the core explain the axial force and rolling moment trends. Side force, yawing moment and normal force show a very sinusoidal behavior, which is due to the freestream velocity vector rotating around the model as it is being rolled. In pitch sweeps, side force normal force and yawing moment all exhibit quite linear trends from -5^o to +5^o, outside of which the slope become steeper. An interesting feature to note is the strong non-linearity of the pitching moment coefficient, and sign reversal around ALPHAV= 0^o, especially visible in Fig. 10. This indicates that the center of pressure is moving forward and aft of the balance moment center through these pitch sweeps at constant PHIV.

E. Transonic shock reflection

The transonic regime is a crucial part of the ascent phase of flight because dynamic pressures are typically very high and launch vehicle controllers usually experience their smallest stability margins around M=1. It is therefore very important to accurately capture the transonic aerodynamics. Unfortunately, due to the presence of walls in a wind tunnel test section, it is also very challenging to acquire interference-free data in the vicinity of M=1. Indeed, just below M=1, increasing blockage effects can impact axial force measurements as the Mach number approaches 1, and above M=1, the very steep angled compression and expansion waves produced on the launch vehicle propagate to the walls and are reflected back onto the model which could significantly corrupt the data. Modern transonic wind tunnels are all equipped with either slotted or perforated test section walls that serve two purposes: to enable the tunnel to get to supersonic Mach numbers without choking, and to minimize the reflected shock intensity.[9] Porous and slotted walls are however a point design and are not optimized for all Mach numbers above 1. Extra vigilance should therefore be exercised when collecting data just above Mach 1.

With a model slightly over 30"-long in this 4-foot square test section, it was estimated that any reflected shock would clear the model above M=1.2. Below M=1.2, there is a possibility that the shock coming off of the nose of the model would reflect back onto the model and corrupt that data. During the Ares I testing in the same tunnel, it was found that reflected shocks did not have an impact on the aerodynamic data, due to the axisymmetric geometry of the vehicle. In the case of SLS however, the large side-mounted boosters act as lifting surfaces and a reflected shock could have a greater impact. By plotting the center of pressure location as a function of Mach number, it was found that unexpected variations were observed between M=0.95 and M=1.30. These can be seen in Fig 12 on the left side. The longitudinal center of pressure location is defined as CLM/CN and is shown at BETA=0^o for various ALPHA angles. The lateral center of pressure location is defined as CLN/CY and is shown at ALPHA=0^o for various BETA angles. Both lateral and longitudinal plots show an oscillation between M=0.95 and 1.30, indicating that a shock is reflecting back onto the model and inducing a shift in the center of pressure. All data at M=1.05, 1.10, and 1.20 was eliminated and replaced with linearly interpolated data between M=0.95 and M=1.30, as shown on the right hand side plots in Fig. 12. To address this issue and ensure the best transonic data quality, several actions were taken by the aerodynamics team: A dedicated transonic test in a large facility is planned with a goal

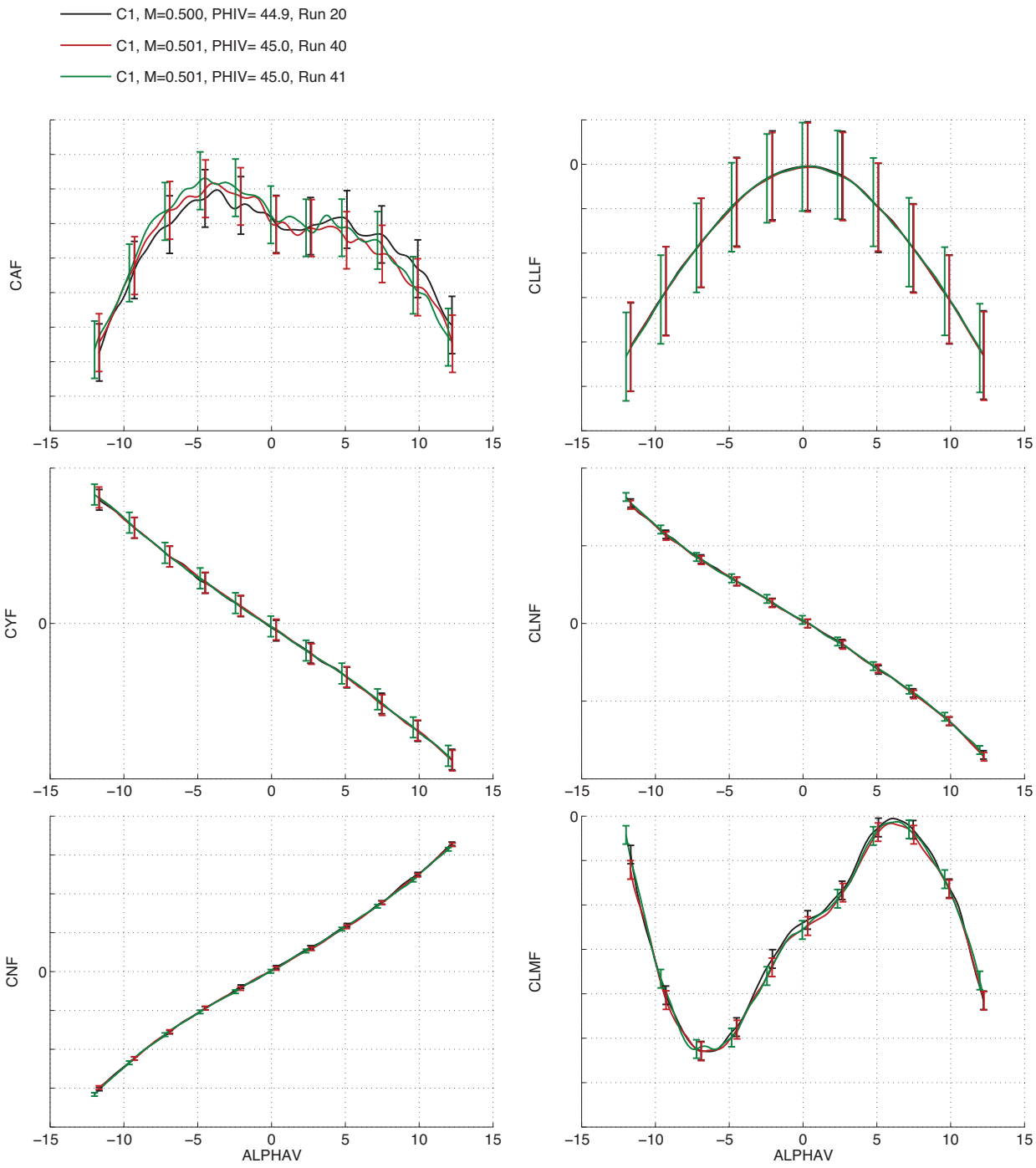

Figure 8. SLS-10003 forebody force and moment coefficients for 3 repeat continuous pitch sweeps at M= 0.5, PHIV= 45°, moment reference at the balance moment center, error bars represent uncertainty due to balance calibration

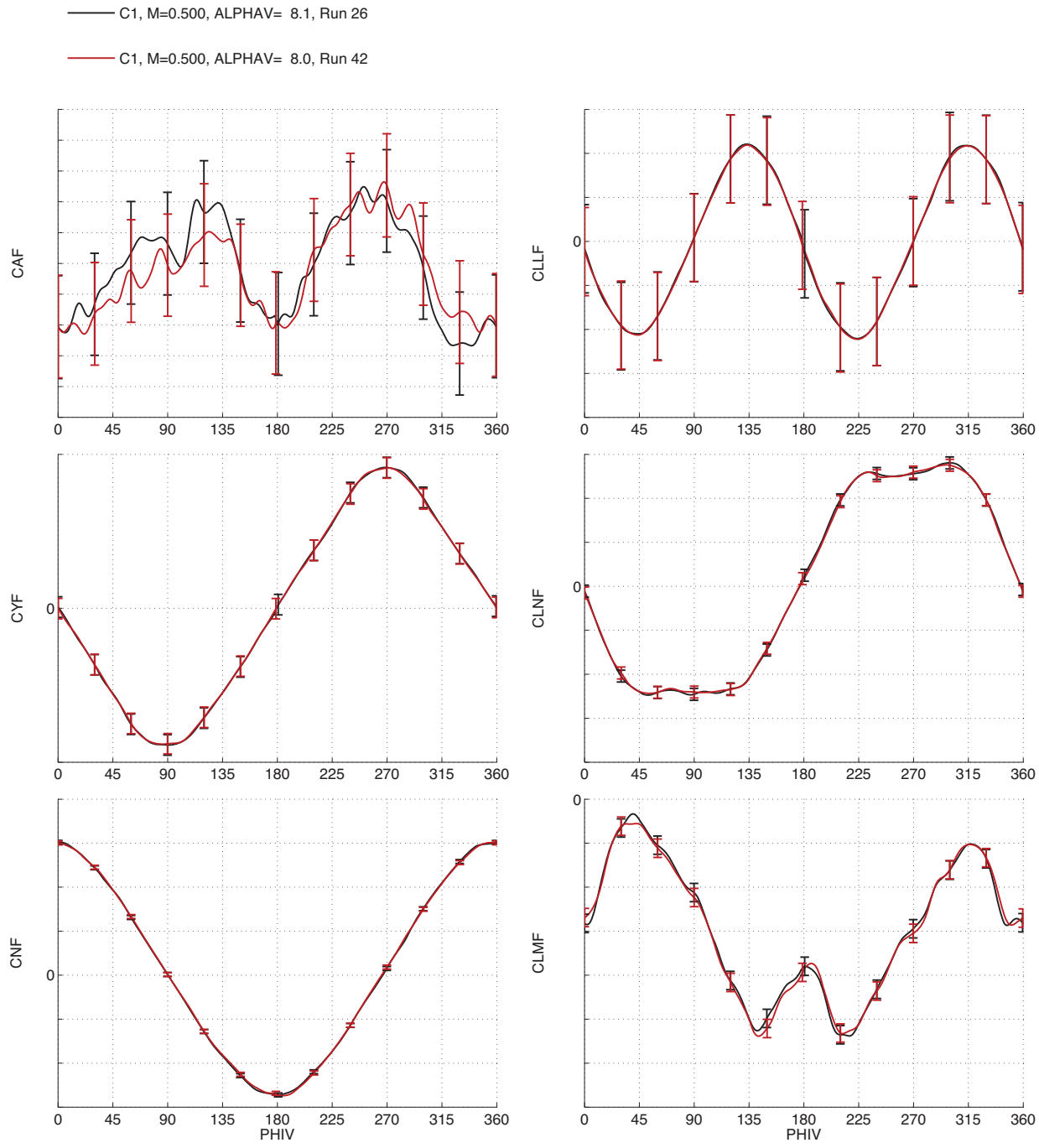

Figure 9. SLS-10003 forebody force and moment coefficients for 2 repeat continuous roll sweeps at M= 0.5, ALPHAV= 8°, moment reference at the balance moment center, error bars represent uncertainty due to balance calibration

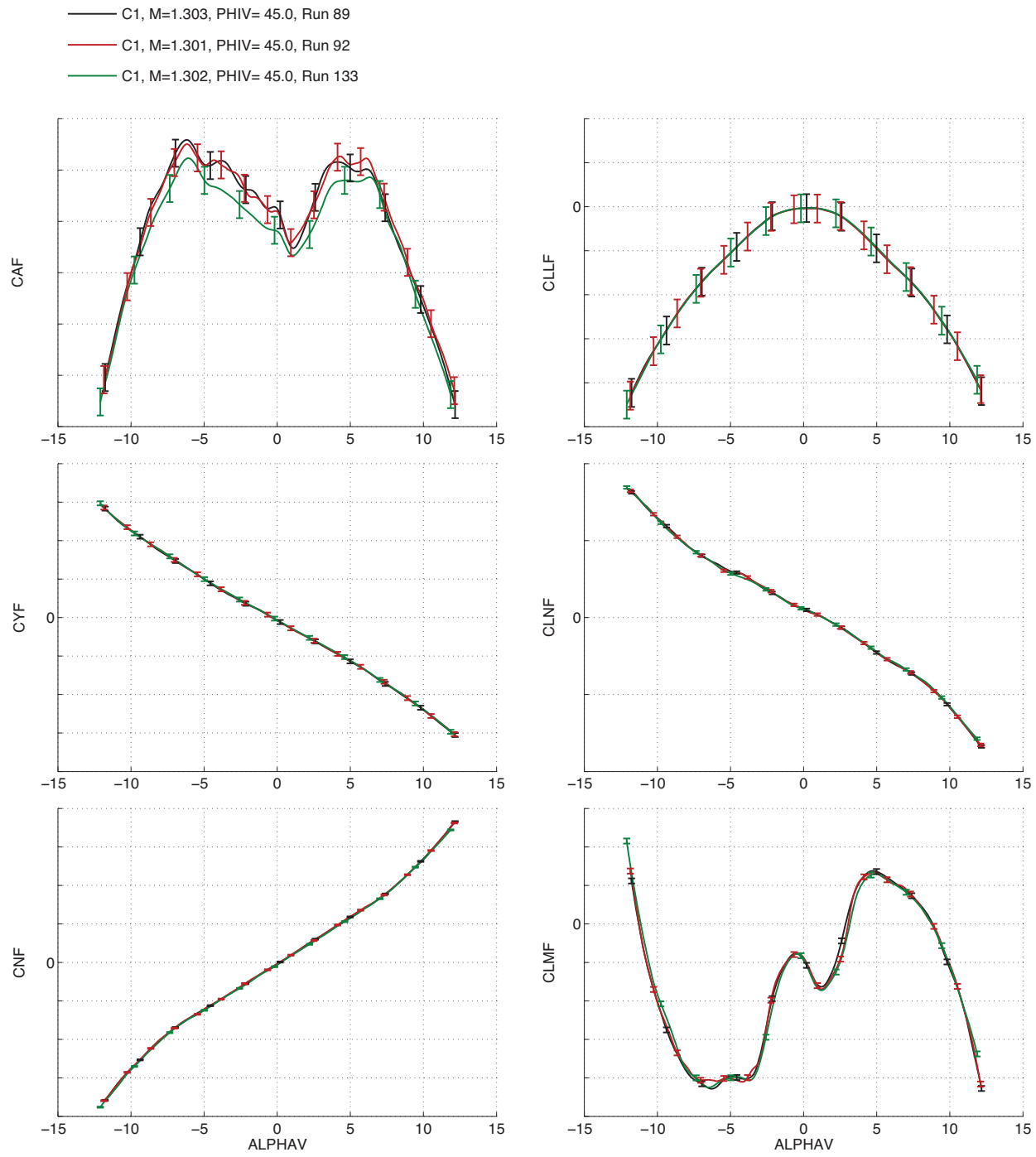

Figure 10. SLS-10003 forebody force and moment coefficients for 3 repeat continuous pitch sweeps at M= 1.3, PHIV= 45°, moment reference at the balance moment center, error bars represent uncertainty due to balance calibration

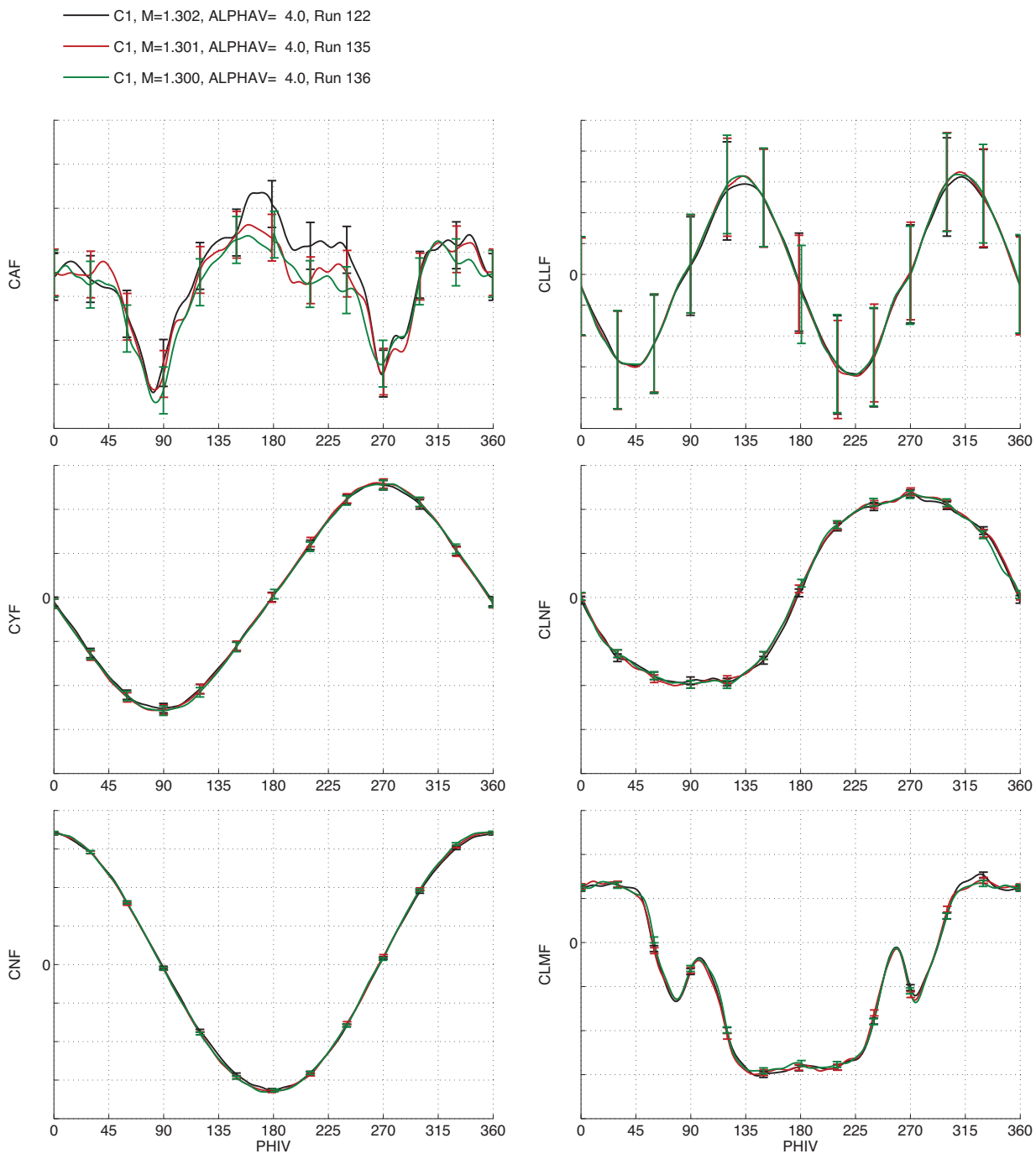

Figure 11. SLS-10003 forebody force and moment coefficients for 2 repeat continuous roll sweeps at M= 1.3, ALPHAV= 8^o, moment reference at the balance moment center, error bars represent uncertainty due to balance calibration

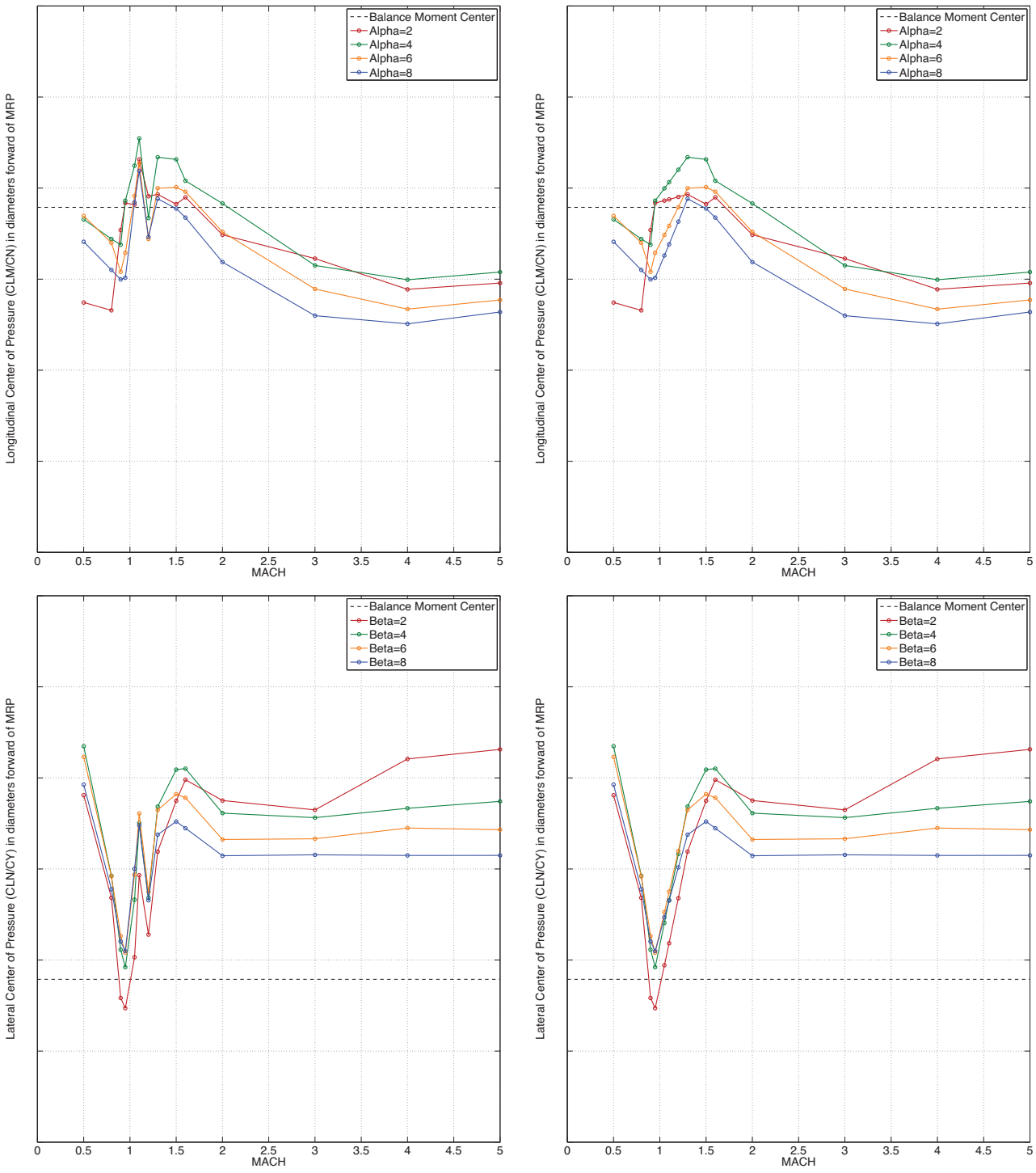

Figure 12. (top) Longitudinal center of pressure location at BETA=0^o, and (bottom) Lateral center of pressure location at ALPHA=0^o as a function of Mach number. Left side plots are *before* linearizing through transonic Mach numbers, right side plots are *after* linearization to correct for shock reflection

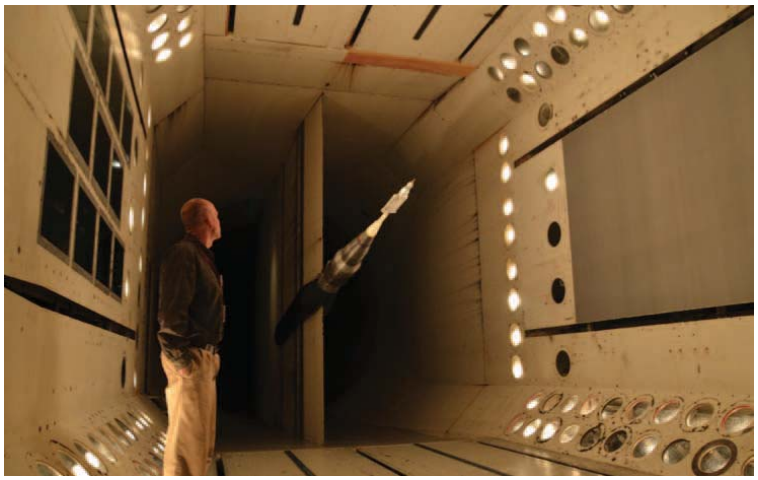

Figure 13. 0.8%-scale SLS model installed in the NASA Langley Transonic Dynamics Tunnel (TDT)

to collect interference-free data through transonic Mach numbers. This test will occur in the summer of 2014. Additionally, a short wind tunnel test of the same model was conducted in NASA Langley's Transonic Dynamics Tunnel (TDT) which has a 16' × 16' test section, and an upper Mach number limit of 1.2. This Mach range was deemed sufficient to assess the validity of the linear interpolation of the PSWT data that was performed through transonic Mach numbers. The blockage ratio in this wind tunnel was 0.027%, which is much lower than the 0.435% blockage ratio in the Boeing PSWT with the same model. The picture in Fig. 13 shows the model installed in the TDT test section. As can be seen in the picture, the test section walls of this transonic tunnel are slotted, and wall interference effects on a small 0.8%-scale model should be minimal. The Reynolds numbers between the two facilities were comparable as well.

Figures 14 and 15 show comparisons of the longitudinal and lateral center of pressure locations from the PSWT data (in red) and the TDT data (in green). Also for reference is shown the previous version of the ascent aerodynamic database (in black), SLS-10-D-AFA-002, which was derived from MSFC 14" TWT wind tunnel data and a 0.4%-scale SLS model. The data are very consistent below M=1, and at M=1.2, however it is clear that the oscillation observed at M=1.10 in the PSWT data is more prominent that in the TDT data. It was therefore concluded that the linear interpolation method was an adequate way to model the transonic aerodynamics, until a more comprehensive transonic test is conducted at a large facility.

II. Database Development

This section describes how the 6-DOF aerodynamic force and moment dataset collected in the wind tunnel was post-processed to produce a formal ascent aerodynamic database.

The SLS-10-D-AFA-003-rev1 database is a third generation force and moment aerodynamic coefficient database generated for use by the SLS trajectory community, and the guidance, navigation and control (GNC) community for ascent design and analysis. Requirements from the data users were to obtain an ascent database that covers Mach numbers from 0.5 to 5, and angles of attack and sideslip from -8^o to +8^o. Due to some of the non-linearities observed around ALPHAV=0^o pointed out in the previous section, the aerodynamics team produced a database with a higher resolution in ALPHA and BETA between -4^o and +4^o, as seen in the following table. This table describes the breakpoints that were produced for the current ascent database:

Variable	SLS-10-D-AFA-003-rev1 Aerodynamic Database Breakpoints
Mach number, M	0.50, 0.80, 0.90, 0.95, 1.05, 1.10, 1.20, 1.30, 1.50, 1.60, 2.00, 3.00, 4.00, 5.00
Angle of attack, ALPHA	-8^o to -4^o every 1^o, -4^o to +4^o every 0.25^o, +4^o to +8^o every 1^o
Sideslip angle, BETA	-8^o to -4^o every 1^o, -4^o to +4^o every 0.25^o, +4^o to +8^o every 1^o

A general recommendation to the users is to linearly interpolate between breakpoints in ALPHA, BETA

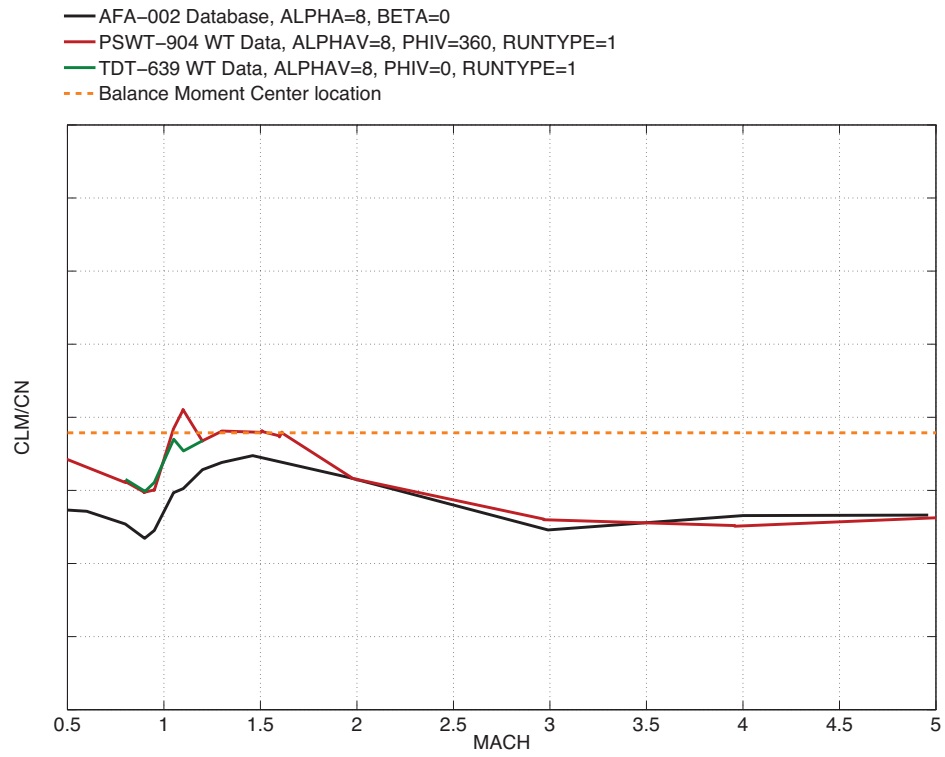

Figure 14. Longitudinal center of pressure location at ALPHAV=8^o, PHIV=0^o as a function of Mach number

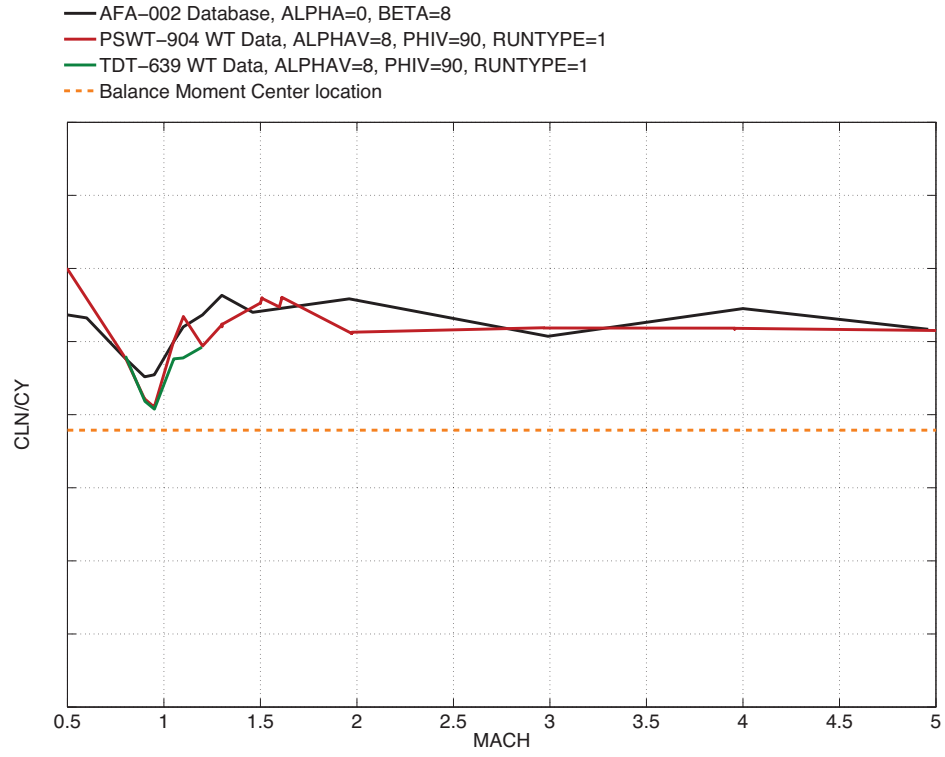

Figure 15. Lateral center of pressure location at ALPHAV=8^o, PHIV=90^o as a function of Mach number

and Mach number. In cases where data is required outside of the provided database, it is recommended to extrapolate linearly outside of the ALPHA and BETA bounds, and to hold last value constant below M= 0.5. Above M= 5.0, linear extrapolation is recommended.

The 6-DOF database is provided in the body axis system, as described in Fig. 7. All aerodynamic coefficients were calculated using a reference length equal to the diameter of the core stage, and a reference surface area equal to the cross-sectional area of the core stage. An arbitrary and standard moment reference point (MRP) is located near the gimbal point of the main engines, below the base of the core stage. All coefficients are provided as forebody coefficients (i.e. base forces and moments removed).

Post-processing of the wind tunnel data and creation of the ascent database was performed entirely using MATLAB. Wind tunnel data post-processing was performed using forebody force and moment coefficients in the body axis system. Since the data was acquired entirely in the pitch plane, the angle of attack/sideslip domain is covered by performing pitch sweeps at a fixed roll angles, and roll sweeps at a fixed pitch angles, at each nominal Mach number. The input domain is therefore filled in the total angle of attack/roll angle space, as shown in Fig. 16 by the black dots. Pitch sweeps were performed from -12^o to +12^o pitch angle. The data at negative pitch angles -12^o to 0^o and fixed roll angle PHIV was re-mapped to pitch angles 0^o to 12^o and roll angle PHIV+180^o. Roll sweeps were performed from PHIV=-180^o to +180^o. The data at negative roll angles -180^o to 0^o was re-mapped to roll angles +180^o to +360^o.

Since the Boeing PSWT is a blow-down facility, the data is acquired in a continuous fashion. The wind tunnel dataset is therefore delivered in very fine pitch and roll increments. To remove some low amplitude noise (well within balance accuracy), a moving-average filter is applied to all pitch and roll sweeps. The data is then interpolated at nominal total angles of attack (from -12^o to +12^o every 0.25^o) and nominal roll angles (from 0^o to 360^o every 5^o). Repeat runs are then averaged to result in a complete and unique set of pitch and roll sweeps. As part of the test matrix, at all Mach numbers, full roll sweeps were performed at 0^o total angle of attack. In the body axis system, all forces and moments should be theoretically constant during such a roll sweep. Some minor systematic biases were thereby measured, and removed during post-processing from all of the data. These systematic biases could come from very small yaw misalignments between the freestream flow and the pitch plane in which the data is acquired. As previously mentioned, the SLS-10003 vehicle, with the presence of all of its protuberances does not present any outer mold line symmetry plane, by which further data corrections could have been applied (as an example, the normal force coefficient data was not forced through zero at a total angle of attack of 0^o). As discussed in the previous section, during post-test data analysis, it was found that at low supersonic Mach numbers, despite wave reflection mitigation techniques being applied during testing, the SLS model was sensitive to shock reflection, and its effects were noticeable in the post-processed dataset. The presence of the two SRBs acting as lifting surfaces, and the SRB aft skirts being at a large distance from the balance moment center, were considered the main reasons for the higher sensitivity of this vehicle to wave reflection than more axisymmetric launch vehicles. After in-depth examination and analysis of the data, including comparisons to historical data and computational simulations, it was decided to replace the M=1.05, 1.10, and 1.20 datasets with data linearly interpolated between M=0.95 and M=1.3. The resulting trends are consistent with those of the previous SLS-10-D-AFA-002-rev2 database, as well as CFD results. Once complete datasets were produced at each nominal Mach number, a multivariate interpolant that implements a natural neighbor interpolation scheme was computed for each coefficient and each Mach number separately. This interpolant was then interrogated at each database angle of attack/sideslip breakpoint combination. Figure 16 shows the interrogation points in the angle of attack/sideslip space (in red).

As an example, Fig. 17 shows the wind tunnel data set (colored dots) and the multivariate interpolant (colored surface) for all 6 force and moment coefficients, at Mach=1.6, as a function of total angle of attack and roll angle. Figure 18 shows the interpolant surface interrogated at each alpha/beta breakpoint (colored dots). Fig. 19 shows these same interrogated data points as a function of ALPHA and BETA. These data points are what constitute the final SLS-10-D-AFA-003-rev1 aerodynamic database at this Mach number of 1.6. The identical process is performed at all Mach numbers.

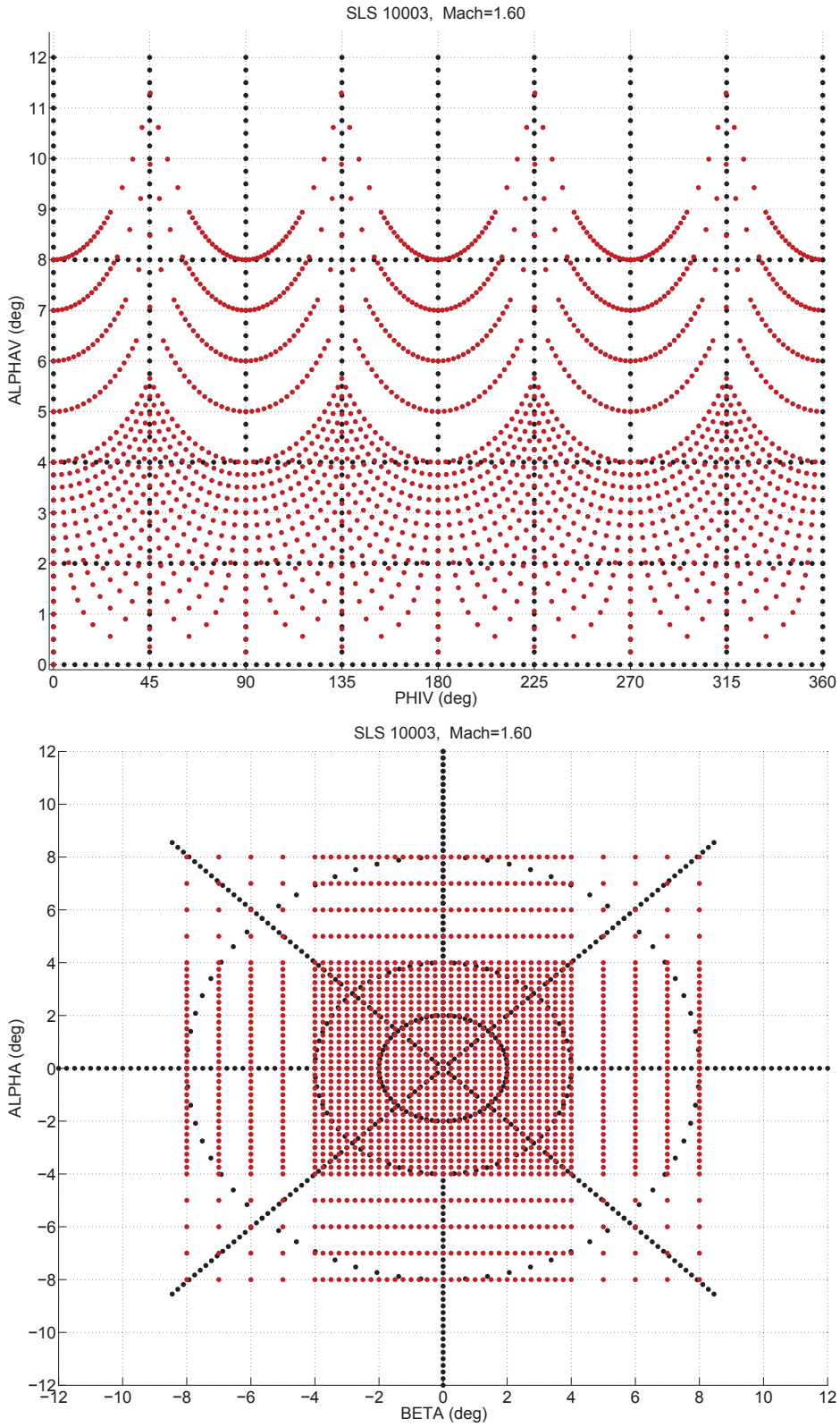

Figure 16. Wind tunnel post-processed data breakpoints (black circles), and database breakpoints (red circles), in the ALPHAV/PHIV space (top) and in the ALPHA/BETA space (bottom)

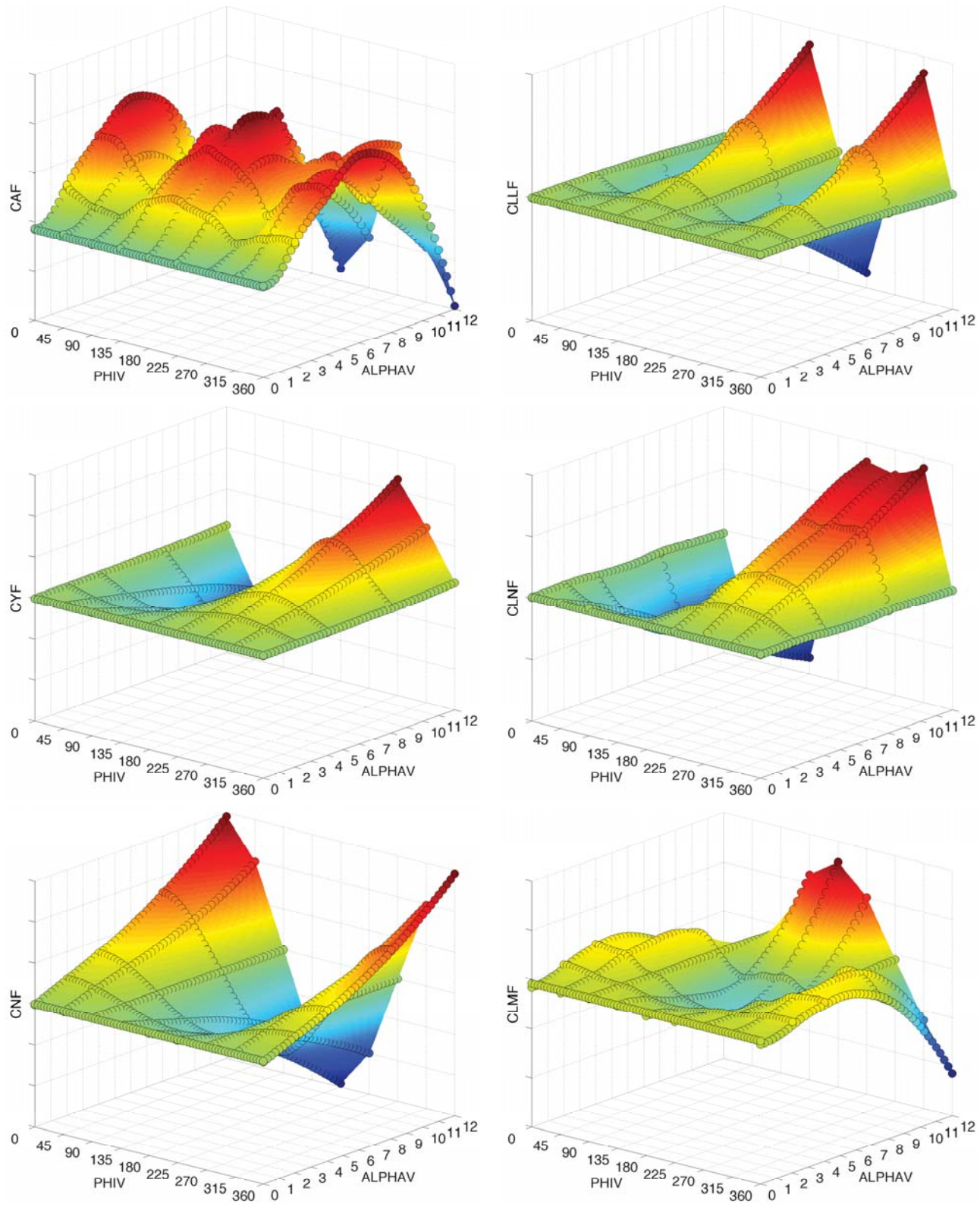

Figure 17. Post-processed forebody force and moment coefficients (symbols), and interpolant surface (color surface), at M= 1.6, moment reference at the balance moment center

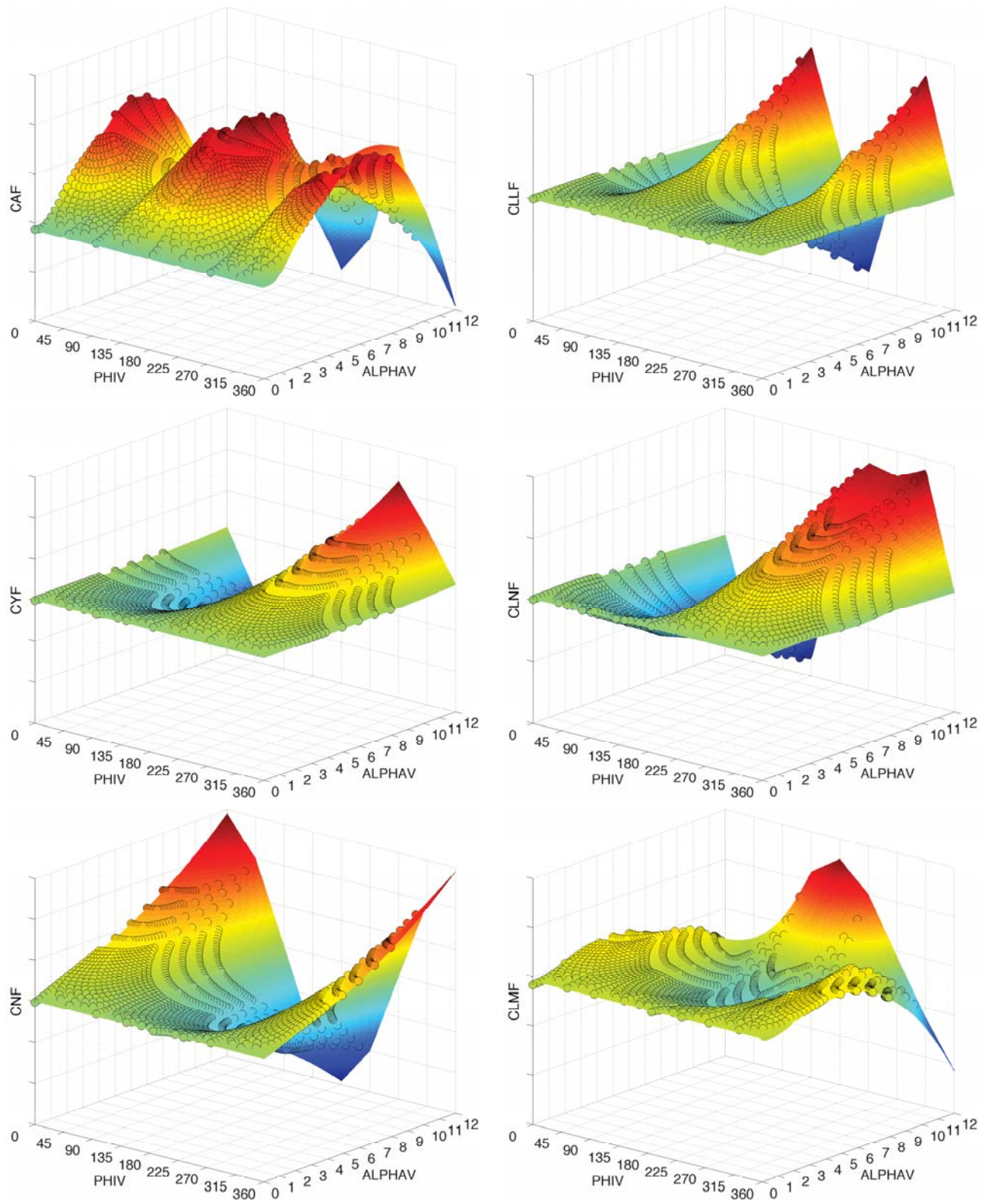

Figure 18. Interpolant surface (color surface), and queried data at database required breakpoints, at M= 1.6, moment reference at the balance moment center

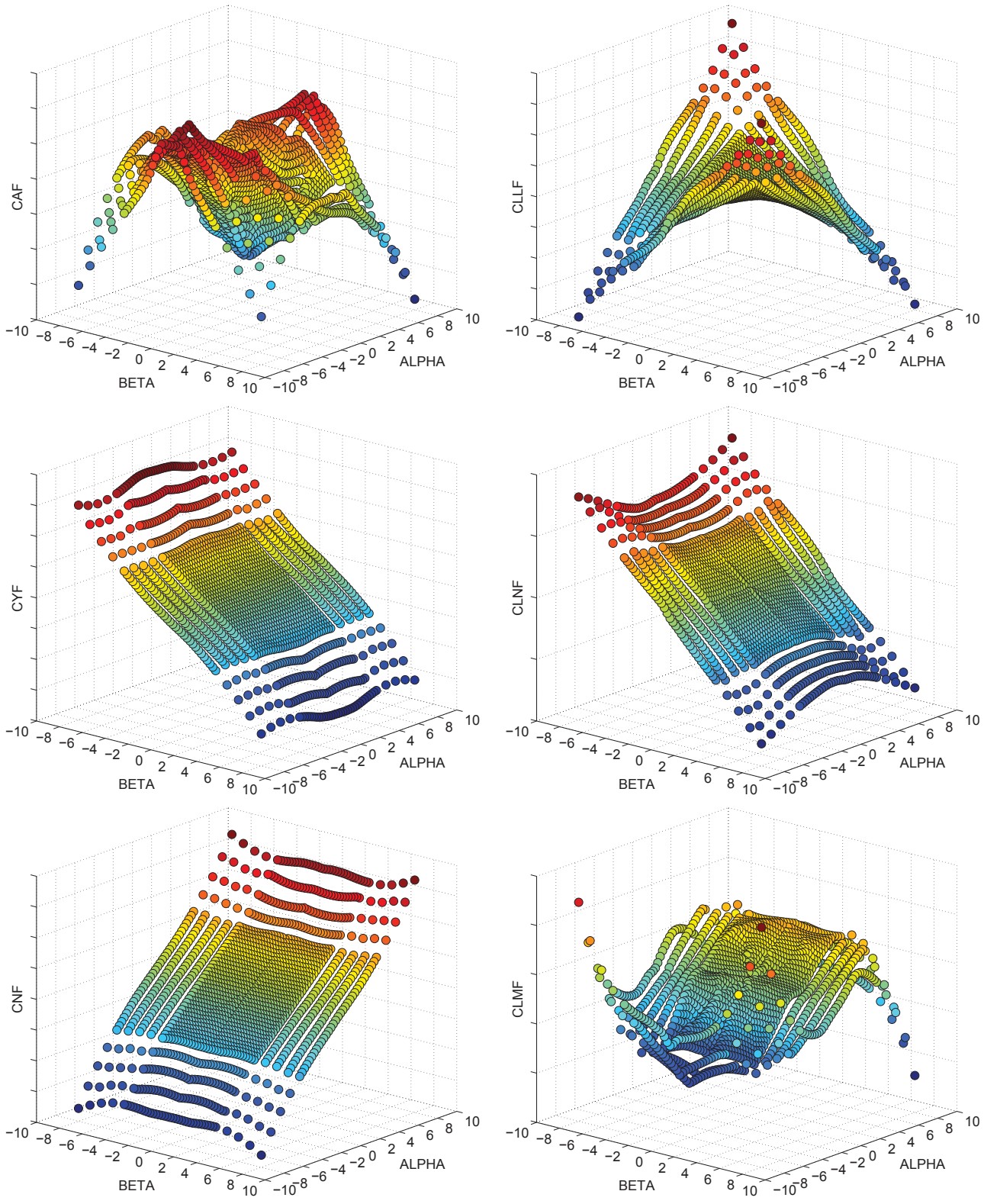

Figure 19. Database forebody force and moment coefficients (symbols), at M= 1.6, moment reference at the balance moment center

III. Conclusion

A 0.8%-scale wind tunnel test was conducted at the Boeing Polysonic Wind Tunnel in St Louis, MO, to collect aerodynamic data for the ascent portion of the flight trajectory of the SLS vehicle, covering a wide Mach range (0.5 to 5). Best practices developed during the Constellation program were followed during all phases of the test. From this wind tunnel dataset, a formal aerodynamic database was created. Due to some concerns over shock reflection effects through transonic conditions, data was linearized between M=0.95 and M=1.3. An upcoming dedicated wind tunnel test will provide high fidelity data for the transonic portion of flight. Once these new transonic data are incorporated into the current database, this will constitute the main ascent aerodynamic database that SLS will utilize for future exploration missions, starting with the first scheduled flight test for 2017.

Acknowledgements

The authors would like to acknowledge the support of the Space Launch System program offices at the NASA Marshall Space Flight Center and at the NASA Langley Research Center.

References

[1]Mayle, M. N., Crosby, W. A., Pritchett, V. E., and Frost, A. L., "Force and Moment Testing of the Space Launch System (SLS) Configurations 10000 and 21000 in the Marshall 14-inch Trisonic Wind Tunnel," *NASA Internal Report, EV33-12-001*, 2011.

[2]Crosby, W. A., Pritchett, V. E., and Mayle, M. N., "Force and Moment Testing of the Space Launch System (SLS) Design Analysis Cycle 2 (DAC2) in the MSFC 14-inch Trisonic Wind Tunnel," *NASA Internal Report, EV33-12-015*, 2012.

[3]Erickson, G. E. and Wilcox, F. J., "Ares I Aerodynamic Testing at the NASA Langley Unitary Plan Wind Tunnel," *49th AIAA Aerospace Sciences Meeting Including the New Horizons Forum and Aerospace Exposition*, AIAA 2011-0999, 2011.

[4]Pinier, J. T., "A New Aerodynamic Data Dispersion Method for Launch Vehicle Design," *Journal of Spacecraft and Rockets*, Vol. 49, No. 5, 2012, pp. 834–841.

[5]"Calibration and Use of Internal Strain-Gage Balances with Application to Wind Tunnel Testing," *AIAA Recommended Practice, AIAA R-091-2003*, 2003.

[6]Hemsch, M. J., Hanke, J. L., Walker, E. L., and Houlden, H. P., "Detailed Uncertainty Analysis for Ares I Ascent Aerodynamics Wind Tunnel Database," *26th AIAA Aerodynamic Measurement Technology and Ground Testing Conference*, AIAA 2008-4259, 2008.

[7]Houlden, H. P., Favaregh, A. L., and Hemsch, M. J., "Quantification of the Uncertainty for the Ares I A106 Ascent Aerodynamic Database," *27th AIAA Aerodynamic Measurement Technology and Ground Testing Conference*, AIAA 2010-4926, 2010.

[8]Montgomery, D. C., *Introduction to Statistical Quality Control*, Third Edition, Wiley, 1996.

[9]Goethert, B. H., *Transonic Wind Tunnel Testing*, Dover Publications, New York, 2007.